Survey of Gravitational Lensing

David Coss*

August 18, 2006

Contents

*drc253@umsl.edu

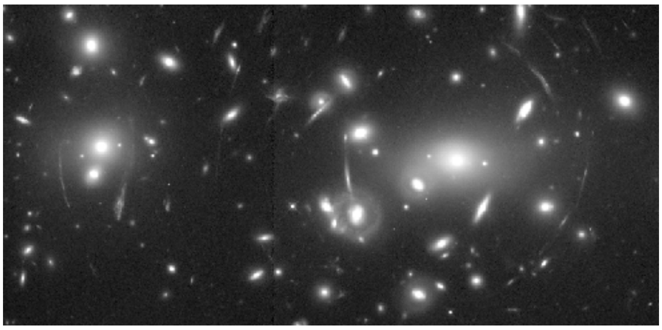

Figure 1: Abell 2218. Picture taken by the Hubble Space Telescope.

1 Introduction

As the title implies, this paper serves as a very general overview of gravitational lensing. My intention is not to write an all inclusive paper. Instead, only what I have recently reviewed has been written. Included in this paper is a collection of formulas, concepts and mathematical functions, which I found either particularly interesting or important in gravitational lensing. Also, there is a list of references, which are either pedagogically helpful, such as Schneider, Ehler, Falco, or historically crucial in lensing and dark matter study, such as Navarro, Frenk, White and many papers by Bartelmann and Schneider. A general theoretical background, mainly using a point-mass lens, is given in Section 2. In Section 3, the Chang-Refsdal Lens is dicussed. The paper is concluded with a discussion of dark matter halos in Section 4. In the appendix, I have made a list of mathematical functions I found useful in lensing study.

2 Theory

2.1 Light Deflection

Before any discussion can be made on light deflection, an appropriate description of the situation must be made, illustrated in Figure 2. In the following section, a light ray will leave the source, S, and travel to the plane of the deflector. The light ray is traveling along r. At the point of deflection, there is a plane perpendicular to r. Within this plane, the position of the light ray is given by the impact vector $\vec{\xi}$, which is a two dimensional vector. More generally, the position of the light ray in three dimensional space is given by the vector $(\vec{\xi}, r)$.

In certain situations, it is advantageous to treat the impact vector as a vector in the complex plane, ie $\vec{\xi} \equiv \xi_1 + i\xi_2$. Aside from its mathematical elegance, complex vectors yield a direct parameterization of critical curves and, through a bit of algebra, caustics (cf. Section 3.4). An excellent overview of complex vectors is given by [20].

If the impact vector, ξ, is much greater than the Schwarzschild radius of the point mass, $R_s \equiv \frac{2GM}{c^2}$, then General Relativity gives a deflection angle given by

$$\hat{\alpha} = \frac{4GM}{c^2\xi} \tag{1}$$

This result is twice the result obtained by Newton mechanics alone.

In a weak gravitational field, the deflection angle for a given impact vector due to a collection of point masses is given by the sum of the deflection angles of each individual mass, analogous to electric fields of point charges.

$$\hat{\vec{\alpha}} = \frac{4G}{c^2}\sum_{i=1}^{N} m(\vec{\xi_i}, r)\frac{\vec{\xi} - \vec{\xi_i}}{|\vec{\xi} - \vec{\xi_i}|^2} \tag{2}$$

For infinitessimal volume elements dV,

$$\hat{\vec{\alpha}} = \frac{4G}{c^2}\int d^2\xi' \int dr' \rho(\vec{\xi'}, r')\frac{\vec{\xi} - \vec{\xi'}}{|\vec{\xi} - \vec{\xi'}|^2}.$$

Since the separation vector $\vec{\xi} - \vec{\xi'}$ is independent of r, the integral over dr' can be replaced by the *surface mass density*

$$\Sigma(\vec{\xi}) \equiv \int dr' \rho(\vec{\xi'}, r'), \tag{3}$$

which is the projection of the mass density ρ onto the plane normal to the light ray at the point of deflection. With this final substitution, the deflection angle is given by

$$\hat{\vec{\alpha}} = \frac{4G}{c^2}\int d^2\xi' \Sigma(\vec{\xi})\frac{\vec{\xi} - \vec{\xi'}}{|\vec{\xi} - \vec{\xi'}|^2} \tag{4}$$

The unprimed factor in this integral suggests that this integral could be written as a gradient, i.e. $\hat{\vec{\alpha}} = \nabla\,\hat{\psi}$, such that

$$\hat{\psi} = \frac{4G}{c^2}\int d^2\xi' \Sigma(\vec{\xi}) \ln|\vec{\xi} - \vec{\xi'}| \tag{5}$$

The deflection angle can also be written in terms of a dimensionless surface mass density, if the surface mass density, Σ, is divided by the critical density

$$\Sigma_{cr} = \frac{c^2}{4\pi G}\frac{D_s}{D_d D_{ds}}, \tag{6}$$

giving

$$\kappa(\vec{\xi}) = \frac{\Sigma(\vec{\xi})}{\Sigma_{cr}}. \tag{7}$$

Then the *scaled* deflection potential and angle become

$$\psi(\vec{\theta}) = \frac{1}{\pi}\int d^2\theta' \kappa(\vec{\theta'}) \ln|\vec{\theta} - \vec{\theta'}| \tag{8}$$

$$\vec{\alpha} = \vec{\nabla}\psi \tag{9}$$

$$\vec{\xi} = D_d\vec{\theta}, \vec{\eta} = D_s\vec{\beta}. \tag{10}$$

Using Equation (74), it can be shown that the potential ψ satisfies the Poisson equation

$$\nabla^2 \psi(\vec{\theta}) = 2\kappa(\vec{\theta}) \ , \tag{11}$$

giving an alternate definition of κ.

2.2 Lens Equations

To mathematically study lensing, it is necessary to have a general equation to map an image position, ξ, to a source position, η. The lens equation can be directly extracted from Fermat's Principle,

$$\nabla \hat{\phi} = 0, \tag{12}$$

where $\hat{\phi}$ is the Fermat potential. Schneider, Ehlers and Falco (1999) give the Fermat potential to be

$$\hat{\phi} = \frac{D_d D_s}{2D_{ds}} \left(\frac{\vec{\xi}}{D_d} - \frac{\vec{\eta}}{D_s} \right)^2 - \hat{\psi}(\vec{\xi}).$$

Substitution into $\vec{\nabla}\hat{\phi} = 0$ with $\hat{\alpha} = \nabla \hat{\psi}$ gives

$$\vec{\eta} = \frac{D_s}{D_d}\vec{\xi} - D_{ds}\hat{\vec{\alpha}}. \tag{13}$$

This is one form of the lens equation.

Due to the scale of the positions involved, it is convenient to write the lens equation with dimensionless quantities, by making the substitution

$$\vec{x} \equiv \frac{\vec{\xi}}{\xi_0} \ , \ \vec{y} \equiv \frac{\vec{\eta}}{\eta_0}. \tag{14}$$

Here, a scale of ξ_0 is used, producing the source scale of $\eta_0 = \xi_0 \frac{D_s}{D_d}$. With these substitutions, the lens equations becomes

$$\vec{y} = \vec{x} - \vec{\alpha}(\vec{x}) \tag{15}$$

2.3 Shear and Convergence

As the gravitational fields involved neither create nor destroy photons, gravitational lensing conserves light intensity. If the flux of the light in the source and image planes is given by $\mathcal{F}_S = I_S d\Omega_S$ and $\mathcal{F}_I = I_I d\Omega_I$. Conservation of intensity, I, gives

$$\frac{\mathcal{F}_I}{\mathcal{F}_S} = \frac{d\Omega_I}{d\Omega_S} = \mu.$$

This is the magnification of the image. Rewriting the solid angles as, $\frac{d\Omega_I}{d\Omega_S} = \frac{d^2x}{d^2y}$, makes it appearent that the magnification can be related to a Jacobian of the mapping of y to x, usually represented by

$$A(\vec{x}) = \frac{\partial \vec{y}}{\partial \vec{x}}. \tag{16}$$

Then the magnification, μ, takes on the familiar form

$$\mu = \frac{1}{det\,A}. \tag{17}$$

One thing becomes very clear with this equation. If $det\,A = 0$, the magnification diverges. Such values of x are called critical points, with corresponding values of y, referred to as caustic points.

Using the Jacobian, A, leads to quantities of particular interest in lensing study: convergence and shear. If $y_i = x_i - (\nabla\,\psi)_i$, then

$$A_{ij} = \delta_{ij} - \frac{\partial^2\psi}{\partial x_i \partial x_j} \tag{18}$$

$$trA = 2 - \frac{\partial^2\psi}{\partial x_1^2} - \frac{\partial^2\psi}{\partial x_2^2} = 2(1-\kappa) \tag{19}$$

$$detA = (1 - \frac{\partial^2\psi}{\partial x_1^2})(1 - \frac{\partial^2\psi}{\partial x_2^2}) - \left(\frac{\partial^2\psi}{\partial x_1 \partial x_2}\right)^2 \tag{20}$$

$$= (1-\kappa)^2 - \left(\frac{\partial^2\psi}{\partial x_1 \partial x_2}\right)^2 - \frac{(\frac{\partial^2\psi}{\partial x_1^2})^2 + (\frac{\partial^2\psi}{\partial x_2^2})^2 - 2\frac{\partial^2\psi}{\partial x_1^2} * \frac{\partial^2\psi}{\partial x_2^2}}{4}. \tag{21}$$

With the determinate of A written as it is in Equation (21), the eigenvalues of A become more clear and compact, if the following substitutions are made:

$$\gamma_1 \equiv \frac{1}{2}(\frac{\partial^2\psi}{\partial x_1^2} - \frac{\partial^2\psi}{\partial x_2^2}) \tag{22}$$

$$\gamma_2 \equiv \frac{\partial^2\psi}{\partial x_1 \partial x_2} \tag{23}$$

$$\gamma^2 \equiv \gamma_1^2 + \gamma_2^2\ . \tag{24}$$

Then the eigenvalues are $1 - \kappa \pm \gamma$. A can now be written as

$$A = \begin{bmatrix} 1-\kappa-\gamma_1 & -\gamma_2 \\ -\gamma_2 & 1-\kappa+\gamma_1 \end{bmatrix}. \tag{25}$$

With this new definition of A, magnification can now also be written in terms of shear, γ, and convergence, κ, as

$$\mu = \frac{1}{(1-\kappa)^2 - \gamma^2} \tag{26}$$

In regions between critical curves, the condition $det\,A \neq 0$ implies there exists an inverse mapping, $\vec{X} = A^{-1}\vec{Y}$, mapping source to an image. In other words, when a source is far enough away from a caustic that the lens equation (15) holds, a source produces *at least* one image. Caustics serve to separate regions of different number of images. In fact, the number of images change by ± 2 if the source crosses a caustic[19].

2.4 Ray Tracing

If a particular model is being analyzed, such that the deflection angle, α, is known, ray tracing may be used to produce a lensed image of a particular source. By inverting the lensing process, points on the lens plane are mapped, or traced, back to the source plane. If the newly found source-plane position corresponds to a position in a source, then there is an image in the lens plane. This process can be carried out easily with the use of a computer[18]. The lens and source planes are divided into a certain number of pixels and the computer scans through them, assigning a lensing magnitude to each image location.

3 Chang-Refsdal Lens

3.1 Background

The Chang-Refsdal lens occurs when a star acts as a point-mass lens, with a surrounding galaxy acting as a perturbation field[8]. This external field makes the Chang-Refsdal Lens different from the so-called Schwarzschild Lens, containing only one point-mass.

3.2 Source and Image as Complex Vectors

Here, the complex vector convention of Witt (1990) and An & Evans (2006) is used because of its simplicity and compactness. To make it obvious when this convention is used, the source and image positions will be represented by ζ and z, respectively. These complex numbers can be related back to the unit vector notation via

$$\zeta \equiv y_1 + \imath y_2 \ , \tag{27}$$
$$z \equiv x_1 + \imath x_2 \ . \tag{28}$$

Due to the symmetry of the mapping of gravitational lensing (Equation 16),

$$\frac{\partial \zeta}{\partial z} = \frac{1}{2}\left(\frac{\partial y_1}{\partial x_1} + \frac{\partial y_2}{\partial x_2}\right) \tag{29}$$

and

$$\begin{aligned} det\, A &= \frac{\partial y_1}{\partial x_1}\frac{\partial y_2}{\partial x_2} - \left(\frac{\partial y_1}{\partial x_2}\right)^2 \\ &= \left|\frac{\partial \zeta}{\partial z}\right|^2 - \left|\frac{\partial \zeta}{\partial \bar{z}}\right|^2 \ . \end{aligned} \tag{30}$$

3.3 Lensing with the Chang-Refsdal Lens

The deflection potential for a point mass is given by

$$\psi = \frac{1}{2}\ln|\vec{x}|^2 \ , \tag{31}$$

since for a point mass, $\Sigma = M\delta^{(2)}(\vec{x})$. Here the point mass has been placed at the origin of the image plane; this is not required, but definitely convenient.

As is mentioned in Section 3.1, the Chang-Refsdal lens is a point-mass in an external field. If the field has mass to cause convergence, the potential is the solution to the Poisson Equation (11). In a mass-free external field, potential is given by the Laplace's Equation, $\nabla^2 \psi_{ext} = 0$. Such a field is studied here.

A solution to the Laplace's Equation is

$$\psi_{ext} = \frac{1}{2}\gamma_1(x_1^2 - x_2^2) + \gamma_2 x_1 x_2 \ , \tag{32}$$

with constants chosen to satisfy Equations (22) - (24). The deflection angle is then the sum of the gradients of the potentials,

$$\vec{\alpha} = \frac{1}{x_1^2 + x_2^2}\vec{x} + \begin{pmatrix} \gamma_1 & \gamma_2 \\ \gamma_2 & -\gamma_1 \end{pmatrix} \vec{x} \ . \tag{33}$$

With this deflection angle for a point mass without convergence, the lensing equation becomes

$$\vec{y} = \vec{x} - \frac{1}{|\vec{x}|^2}\vec{x} - \begin{pmatrix} \gamma_1 & \gamma_2 \\ \gamma_2 & -\gamma_1 \end{pmatrix} \vec{x} \ , \tag{34}$$

or in complex notation

$$\zeta = z - \frac{1}{\overline{z}} - \gamma\overline{z} \ , \tag{35}$$

where $\gamma = \gamma_1 + \imath\gamma_2$. Magnification with this lens equation is $\frac{1}{det\,A}$, (cf. Equation (30)), or

$$\mu = \frac{1}{1 - \left|\frac{1}{z^2} - \overline{\gamma}\right|^2} \ . \tag{36}$$

3.4 Critical Curves

By definition, critical curves are values of z where magnification diverges, Equation (36). Witt (1990) reiterates that because $a^2 = b\bar{b}$, Equation (71), setting the Jacobian of the lens mapping equal to zero gives

$$\frac{1}{z^2} - \overline{\gamma} = e^{-2\imath\varphi} \ . \tag{37}$$

In solving for z, it is important to note a branch-cut exists when evaluating the square root of the complex number in Equation (37). To work around this branch-cut, the critical curves are evaluated in two regions, when $0 \leq |\gamma| < 1$ and $|\gamma| > 1$. Within these regions,

$$z_{cc} = \begin{cases} \dfrac{e^{\imath\varphi}}{(1 + \overline{\gamma}e^{2\imath\varphi})^{\frac{1}{2}}} & , \quad 0 \leq |\gamma| < 1 \\ \pm\gamma^{-\frac{1}{2}}(1 + \overline{\gamma}^{-1}e^{-2\imath\varphi})^{-\frac{1}{2}} & , \quad |\gamma| > 1 \end{cases} \ . \tag{38}$$

z_{cc} can be written in the direction of shear, with the substitution $\gamma = |\gamma|e^{2\imath\varphi_\gamma}$ and $\tilde{\varphi} = \varphi - \varphi_\gamma$,

$$z_{cc} = \begin{cases} \frac{e^{\imath\tilde{\varphi}}}{(1+|\gamma|e^{2\imath\tilde{\varphi}})^{\frac{1}{2}}} e^{\imath\varphi_\gamma} & , \quad 0 \leq |\gamma| < 1 \\ \\ \pm\frac{1}{(|\gamma|+e^{-2\imath\tilde{\varphi}})^{\frac{1}{2}}} e^{\imath\varphi_\gamma} & , \qquad |\gamma| > 1 \end{cases} . \tag{39}$$

4 Study of Dark Matter Halos

4.1 Necessity of Dark Matter Halos

There are various reasons for the proposition of the existence of dark matter. The one of particular interest here is to account for unseen mass formed around galaxies.

When the velocities of stars within the outer rim of galaxies are measured, they are much higher than expected. Tangential velocity of an object moving under the influence of gravity of an object of mass, $M(r)$, is given by

$$\frac{mv^2}{r} = \frac{G_N m M(r)}{r^2} \Rightarrow v = \sqrt{\frac{G_N M(r)}{r}}. \tag{40}$$

This can be summarized as,

$$v \propto \begin{cases} r\,,\ within\, M(r) \\ r^{-\frac{1}{2}}\,,\ outside\, M(r) \end{cases} \tag{41}$$

as shown in Figure 3. However, *observed* velocities remain constant once the maximum value is reached. Therefore, there must be some mass in addition to the visible galaxy keeping the outer stars in circular motion. Dark matter accounts for this mass.

Dark matter is dark because, electromagnetically, it interacts weakly, if at all. According to current cosmological models, in the current epoch, matter content is about 30% of the critical density[9],

$$\rho_c = \frac{3H^2(z)}{8\pi G_N}. \tag{42}$$

It is often advantageous to write the density as a ratio with respect to the critical density,

$$\Omega \equiv \frac{\rho}{\rho_c}. \tag{43}$$

For example, matter has a density ratio of $\Omega_M = 0.3$; most of which is dark matter.

4.2 Alternative to Dark Matter

Introduced by Mordehai Milgrom[16] in the early 1980's, Modified Newtonian Dynamics (MOND) attempts to solve puzzles in cosmology, such as rotation curves, without "the need to assume large amounts of hidden mass in galaxy systems." According to MOND, gravitational forces follow Newton's force law, $F \propto \frac{1}{r^2}$, only on acceleration scales at least that of the solar system. Outside of this realm, a modification of the gravitational potential in the Poisson equation is necessary. One advantage of this theory is it reproduces rotation curves without the need of dark matter. However, it has been shown by Clowe et al (2004) that even in a cosmology including MOND, some mass must be dark matter. Since MOND has no basis is general relativity, MOND cannot be used with weak lensing to measure mass. Regardless, two cases force dark matter to be included. First, Clowe et al (2004) point out that MOND cannot account for the difference in shear in systems with and without x-ray peaks without dark matter included. Hoekstra et al (2004) show that MOND predict isotropic lensing, which they excluded with 99.5% confidence (cf Section 4.4). Though these tests have not ruled out MOND altogether, ironically, they have shown that it must include dark matter.

4.3 Cold Dark Matter versus Hot Dark Matter

Dark matter can be classified by its energy. Hot dark matter (e.g. neutrinos) has low mass but relativistic energy. Cold dark matter, on the other hand, is more massive with less energy. Hot and cold dark matter differ in the way in structures are formed.

Due to their high energy and lack of electromagnetic interaction, hot dark matter particles would race through regions in space with high density. It would therefore take large, already present structures to capture dark matter, as we see them around galaxies. In other words, large scale structures would have been produced first, contrary to observation[11].

It appears that small scale structures appear first. Once halos became large enough, Hydrogen began to clump. Hydrogen and Helium could then condense within this halo. Such a process is supported by cold dark matter, not hot dark matter. Therefore cold dark matter won the right to be included in the cosmological model[11].

4.4 Dark Matter Halo Shape

One major application of gravitational lensing is to evaluate the mass density profiles of unseen galaxy halos. Various density profiles have been proposed; three of which are summarized here.

The simplest profile is the Singular Isothermal Sphere, or SIS. SIS is a helpful illustrative model, due to its simplicity. Similar to the Schwarzschild lens, it assumes a great deal of symmetry, making it inaccurate in real situations. The surface density is given by[19]

$$\Sigma(r) = \frac{\sigma^2}{2G}\frac{1}{r} \tag{44}$$

where σ is the dispersion velocity of the system. An obvious problem with this model is the singularity at $r = 0$. However, the model becomes less problematic at larger scales. If a scale of

$$\xi_0 = 4\pi \left(\frac{\sigma}{c}\right)^2 \left(\frac{D_{ls} D_l}{D_s}\right) \tag{45}$$

is used, the lens equations becomes,

$$y = x - \frac{x}{|x|} \ . \tag{46}$$

The Truncated Isothermal Sphere (TIS), first proposed by Brainerd et al (1996), is similar to SIS, only including a scale by which the profile is truncated. In this model, the mass density is given by

$$\rho(r) = \frac{\sigma^2 s^2}{2\pi r^2 (r^2 + s^2)} \ , \tag{47}$$

where s is the truncation scale.

In 1996, Navarro, Frenk and White[17] proposed the density profile,

$$\rho(r) = \frac{\delta_c \rho_c}{\left(\frac{r}{r_s}\right)\left(1 + \frac{r}{r_s}\right)^2} \ , \tag{48}$$

which is now know as the NFW profile. The NFW profile, like the TIS, has a distance scale, r_s. Unique to the NFW is the density contrast parameter,

$$\delta_c = \frac{200c^3}{3\left(\ln(1+c) - \frac{c}{1+c}\right)} \ , \tag{49}$$

where $c \equiv \frac{r_{200}}{r_s}$. Within the radius r_{200}, the density is equal to 200 times the critical density, ρ_c. This is the Virial radius, which corresponds to a Virial mass of

$$M_{200} = \frac{800\pi r_{200}^3}{3} \rho_c(z) \ . \tag{50}$$

On small scales the NFW profile has some difficulty, but on large scales it works well[13].

Based on simulations, galaxy halos have been shown to be ellipsoidal, of varying degrees. Comparisons of axial ratios of halos provide a method of studying halo shape. For such a comparison, the axes are label, from largest to smallest, as a, b, c, and ratios are defined as $s \equiv \frac{c}{a}$, $q \equiv \frac{b}{a}$ and $p \equiv \frac{c}{b}$. Allgood et all (2006) found the average smallest-to-largest ratio to be well described by

$$< s >= 0.54 \left(\frac{M_{vir}}{M_*}\right)^{-0.050} \ . \tag{51}$$

This relation is given at $R \approx 0.3R_{vir}$. At larger radii, halo shapes become more spherical, with their rates increasing as the mass of the halos increase.

Redshift and σ_8 dependencies were shown by Allgood et al (2006) to still be well described by (51), with their influence found in the value of M_*, which is a characteristic mass at that redshift.

Another interesting feature of halo shape is its alignment and ellipticity compared with the luminous galaxy. Two papers in particular, [13] and [15], study the ellipticity of dark matter halos, using galaxy-galaxy lensing. A necessary definition is

$$f \equiv \frac{e_h}{e_g} , \tag{52}$$

which is the ratio of the ellipticities of the halo and galaxy. According to Hoekstra et al (2004), $f = 0.77^{+0.18}_{-0.21}$, where spherical haloes, $f = 0$, where excluded with 99.5% certainty. Mandelbaum et al (2005), however, differentiate between spiral and elliptical galaxies, vial photometric redshift data not available in the Hoekstra et al (2004) study. Their values are $f = 0.1 \pm 0.06$ and $f = -0.8 \pm 0.4$ for elliptical and spiral galaxies, respectively. Here they have assumed a power law density profile. If a "more realistic"[15] NFW profile is used the values change to $f = 0.6 \pm 0.38$ and $f = -1.4^{+1.7}_{-2.0}$ for elliptical and spiral galaxies, respectively. As for alignment, though dark matter halos are not believed to be supported by rotation, it has been shown that angular momentum and the small axis, c, are well aligned[1].

A Mathematical Functions

A.1 Cauchy Integral Formula

Let $f : \mathbb{C} \to \mathbb{C}$ be analytic on and within the contour C. Then for any point z_0 within C

$$f(z_0) = \frac{1}{2\pi\imath}\oint_C \frac{f(z)}{z - z_0} dz \tag{53}$$

This is a consquence of the Cauchy-Goursat Theorem[12]: $\oint_C f(z)dz = 0$, if f(z) is analytic on and within C.

A.2 Fourier Analysis

For a function, $f(t)$, defined on the interval (a, b), let $T \equiv b - a$, then the Fourier Series of $f(t)$ is given by

$$f(t) = \frac{1}{\sqrt{T}} \sum_{n=-\infty}^{\infty} f_n e^{2\pi\imath nt/T} \ , \tag{54}$$

where

$$f_n = \frac{1}{\sqrt{T}} \int_a^b e^{-2\pi\imath nt/T} f(t) dt \ . \tag{55}$$

If the Fourier series of a real function is being found, it is natural to use trigonometric functions instead of exponential. In which case, the Fourier series takes on the more familiar form,

$$f(t) = \frac{1}{2}A_0 + \sum_{n=1}^{\infty}\left(A_n \cos(\frac{2n\pi t}{T}) + B_n \sin(\frac{2n\pi t}{T})\right) \ , \tag{56}$$

where

$$A_n = \frac{2}{T}\int_a^b \cos(\frac{2n\pi t}{T}) f(t) \tag{57}$$

$$B_n = \frac{2}{T}\int_a^b \sin(\frac{2n\pi t}{T}) f(t) \ . \tag{58}$$

For functions which are not periodic, the Fourier Transform must be used instead of the Fourier Series.The Fourier Transform of $f(x)$ is

$$\tilde{f}(k) = \frac{1}{\sqrt{2\pi}} \int_{-\infty}^{\infty} f(x) e^{-\imath kx} dx \ . \tag{59}$$

The inverse if given by

$$f(x) = \frac{1}{\sqrt{2\pi}} \int_{-\infty}^{\infty} \tilde{f}(k) e^{\imath kx} dk \ . \tag{60}$$

The Fourier transform can be generalized to n-dimensions by:

$$\tilde{f}(\vec{k}) = \frac{1}{\sqrt{2\pi}^n} \int d^n x e^{-i\vec{k}\cdot\vec{r}} f(\vec{r}) \tag{61}$$

$$f(\vec{r}) = \frac{1}{\sqrt{2\pi}^n} \int d^n k e^{i\vec{k}\cdot\vec{r}} \tilde{f}(k) \ . \tag{62}$$

It is worth noting that for $f(x)$, only the exponential contains x. This makes Fourier transform very useful with differential equations, since

$$\frac{df(x)}{dx} = \frac{\imath}{\sqrt{2\pi}} \int_{-\infty}^{\infty} k\tilde{f}(k) e^{\imath kx} dk \ . \tag{63}$$

A.3 Gamma Function

As a definite integral:

$$\Gamma(z) = \int_0^\infty t^{z-1} e^{-t} dt \quad = 2 \int_0^\infty e^{-t^2} t^{2z-1} dt \ \ \forall z \in \mathbb{C}, Re(z) > 0 \tag{64}$$

Gamma is analytic $\forall z \in \mathbb{C}$, having residue at $z \in \mathbb{Z} \backsim \mathbb{Z}^+$ given by

$$\underset{z=-k}{Res}\, \Gamma(z) = \frac{(-1)^k}{k!} \tag{65}$$

Also, Gamma may be written recursively [12]

$$\Gamma(z+1) = z\Gamma(z) \tag{66}$$

or related to the factorial as $\Gamma(n) = (n-1)!\ ,\ \ \forall n \in \mathbb{Z}^+$.

A.4 Hypergeometric Function

$$F(\alpha, \beta; \gamma; z) =_2 F_1(\alpha, \beta; \gamma; z) \equiv \sum_{k=0}^{\infty} a_k z^k \tag{67}$$

where $a_0 = 1$ and

$$a_{k+1} \equiv \frac{(\alpha+k)(\beta+k)}{(k+1)(\gamma+k)} a_k \ \forall k \geqslant 0$$

If γ is positive, this can be written as a series:

$$F(\alpha, \beta; \gamma; z) = \frac{\Gamma(\gamma)}{\Gamma(\alpha)\Gamma(\beta)} \sum_{k=0}^{\infty} \frac{\Gamma(\alpha+k)\Gamma(\beta+k)}{\Gamma(k+1)\Gamma(\gamma+k)} z^k \tag{68}$$

The Geometric Series is the case $F(1, \beta; \beta; z)$

${}_2F_1(\alpha, \beta; \gamma; z)$ is one specific case of the hypergeometric series which can be expanded for an arbitrary number of parameters as:

$${}_pF_q(a_0, a_1, \ldots, a_p; b_0, b_1, \ldots, b_q; z) \equiv \sum_{k=0}^{\infty} a_k z^k$$

where $a_0 = 1$ and

$$a_{k+1} \equiv \frac{\prod_{i=0}^{p}(a_i+k)}{(k+1)\prod_{j=0}^{q}(b_j+k)} a_k \ \forall k \geqslant 0 \tag{69}$$

A.5 Laurent Series

Let $z \in \mathbb{C}$ and $f : S \mapsto \mathbb{C}$ be analytic in $S \subset \mathbb{C}$.

$$f(z) = \sum_{n=-\infty}^{\infty} a_n (z - z_0)^n \tag{70}$$

where $a_n = \frac{1}{2\pi\imath} \oint_S \frac{f(\zeta)}{(\zeta - z_0)^{n+1}} d\zeta$.

It is worth noting:

- $\oint_S f(z)dz = 2\pi\imath a_{-1}$. This value, a_{-1}, is the Residue of f(z) at some singular point z_0, represented by $\oint_S f(z)dz = 2\pi\imath Res[f(z_0)]$.
- If there are multiple singular points in a series, then the integral may be found by a sum of residues. Namely, $\oint_S f(z)dz = \sum_{n=1}^{N} \oint_{S_n} f(z)dz = 2\pi\imath \sum_{n=1}^{N} Res[f(z_n)]$, where N is the number of singular points within S.

A.6 Various Identities

Complex Numbers

$$a^2 = b\bar{b} \Rightarrow b = ae^{i\varphi} \quad \forall a \in \mathbb{R}, b \in \mathbb{C}, \varphi \in [0, 2\pi] \tag{71}$$

Complex Vectors

Let $\vec{a} \equiv \begin{pmatrix} \xi \\ \eta \end{pmatrix}$ and $\vec{b} \equiv \begin{pmatrix} x \\ y \end{pmatrix}$, and $\zeta \equiv \xi + \imath\eta$, $z \equiv x + \imath y$, where $\xi, \eta, x, y \in \mathbb{R}$, then

$$\vec{a} \cdot \vec{b} = \frac{1}{2}(\zeta\bar{z} + \bar{\zeta}z) \tag{72}$$

and

$$|\vec{a} \times \vec{b}| = \frac{\imath}{2}[\zeta\bar{z} - \bar{\zeta}z] \tag{73}$$

Note: Equation (73) gives only the magnitude of the cross product since the direction requires the definition of a basis orthogonal to both the Real and Imaginary axes. Though one *could* be defined, *only* the complex plane is being used. Since such a basis is not necessary, it is not defined. The magnitude of the cross product, however, may be interesting, as it gives the area of a parallelogram created by the two vectors, $\vec{a}$ and $\vec{b}$. Derivation of dot and cross products are given in [7].

Dirac Delta Function

For a 2-D vector, $\vec{x}$,

$$\nabla^2 \ln |\vec{x}| = 2\pi\delta^{(2)}(\vec{x}) \ . \tag{74}$$

$\delta(x - x')$ may also be represented as,

$$\delta(x - x') = \frac{1}{2\pi} \int_{-\infty}^{\infty} e^{\imath k(x-x')} dk \ , \tag{75}$$

or, more generally, for n-dimensions

$$\delta(\vec{x} - \vec{x'}) = \frac{1}{(2\pi)^n} \int_{-\infty}^{\infty} e^{\imath\vec{k}\cdot(\vec{x}-\vec{x'})} d^n k \ . \tag{76}$$

Hypergeometric Function

$${}_2F_1(a, b; c; x) - {}_2F_1(a-1, b; c; x) = x\frac{b}{c}\,{}_2F_1(a, b+1; c+1; x) \tag{77}$$

Proof given in [7].

References

[1] Allgood, B., Flores, R., Primack, J., Kravtsov, A., Wechsler, R., *The Shape of Dark Matter Halos: Dependence on Mass, Redshift, Radius and Formation*, 2006, MNRAS, 367, 1781.

[2] An, J., Evans, N., *The Chang-Refsdal Lens Revisited*, 2006, MNRAS, 369, 317.

[3] Bartelmann, M., *Applications of Gravitational Lensing in Cosmology*, http://www.ub.uni-heidelberg.de/archiv/5962.

[4] Bartelmann, M., Schneider, P., *Weak Gravitational Lensing*, 1999, astro-ph/9912508.

[5] Bourassa, R., Kantowski, R., *The Theory of Transparent Gravitational Lenses*, 1975, ApJ, 195, 13.

[6] Brainerd, T., Blandford, R., Smail, I., *Weak Gravitational Lensing by Galaxies*, 1996, ApJ, 466, 623.

[7] Coss, D., *Various Proofs and Derivations*, 2006, http://www.umsl.edu/˜drc253/research/proofs.pdf.

[8] Chang, K., Refsdal, S., *Star Disturbances in Gravitational Lens Galaxies*, 1984, A&A, 132, 168.

[9] Cheng, T.P., *Relativity, Gravitation and Cosmology: A Basic Introduction*, 2005, Oxford University Press: New York.

[10] Clowe, D., Gonzalez, A., Markevitch, M., *Weak Lensing Mass Reconstruction of the Interactive Cluster 1E0657-558: Direct Evidence for the Existence of Dark Matter*, 2004, ApJ, 604, 596.

[11] Frank, A., *The First Billion Years*, June 2006, Astronomy, 30.

[12] Hassani, S., *Mathematical Physics*, 1999, Springer-Verlag: New York.

[13] Hoekstra, Yee, H., Galdders, M., *Properties of Galaxy Dark Matter Halos from Weak Lensing*, 2004, ApJ, 606, 67.

[14] Kaiser, N., Squires, G., *Mapping the Dark Matter with Weak Gravitational Lensing*, 1993, ApJ, 404, 441.

[15] Mandelbaum, R., Hirata, C., Broderick, T., Seljak, U., Brinkmann, J., *Ellipticity of Dark Matter Halos with Galaxy-Galaxy Weak Lensing*, 2006, MNRAS, 368, 715.

[16] Milgrom, M., *A Modification of the Newtonian Dynamics*, 1983, ApJ, 270, 384.

[17] Navarro, J., Frenk, C., White, S., *The Structure of Cold Dark Matter Halos*, 1996, ApJ, 462, 563.

[18] Newbury, P., Spiteri, R., *Inverting Gravitational Lenses*, 2002, SIAM, 44, 111.

[19] Schneider P., Ehlers, J., Falco, E. E., *Gravitational Lenses*, 1999, Springer-Verlag: New York.

[20] Witt, H. J., *Investigation of high amplification events in light curves of gravitational lensed quasars*, 1990, A&A, 236, 311.

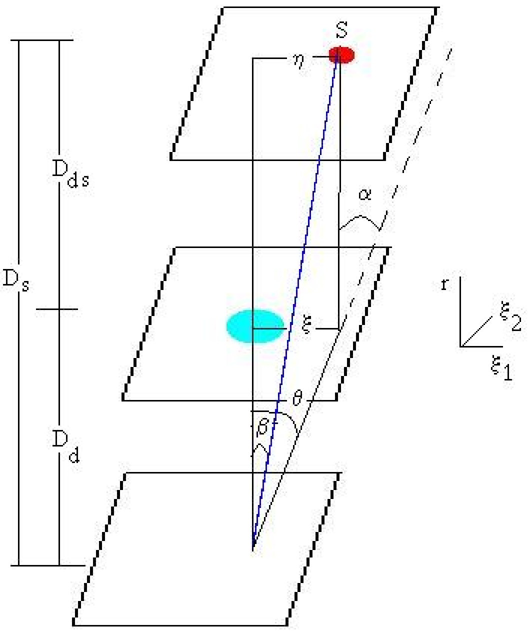

Figure 2: Point-mass Lensing. Light from the Source, S, is deflected by the lens, producing and image at ξ. Within the source plane, the deflected image is away from the undeflected image (blue line) by an angle α

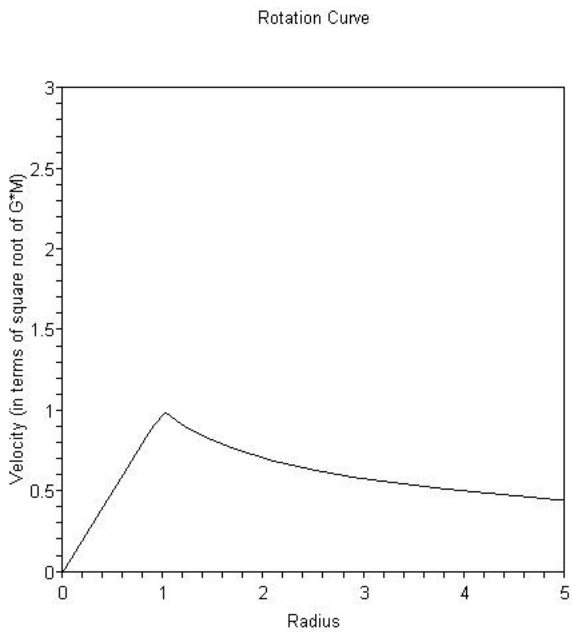

Figure 3: Rotation Curve for a star in circular motion. The velocity and radius are given in terms of $\sqrt{G_N M(r)}$.